Geochemistry, Geophysics, Geosystems

RESEARCH ARTICLE
10.1029/2020GC009608

Key Points:

- Degassing of Tl from experimental melts are associated with kinetic isotope fractionation limited by diffusion in the gas phase
- Basaltic lavas from Kamchatka follow the same Tl depletion-isotope fractionation pattern as experimental charges
- The majority of literature Tl isotope data for volcanic lavas reveal only limited effects from degassing

Correspondence to:
S. G. Nielsen,
snielsen@whoi.edu

Citation:
Nielsen, S. G., Shu, Y., Wood, B. J., Blusztajn, J., Auro, M., Norris, C. A., & Wörner, G. (2021). Thallium isotope fractionation during magma degassing: Evidence from experiments and Kamchatka arc lavas. *Geochemistry, Geophysics, Geosystems*, *22*, e2020GC009608. https://doi.org/10.1029/2020GC009608

Received 18 DEC 2020
Accepted 6 APR 2021

Thallium Isotope Fractionation During Magma Degassing: Evidence From Experiments and Kamchatka Arc Lavas

Sune G. Nielsen[1,2], Yunchao Shu[1,3], Bernard J. Wood[4], Jerzy Blusztajn[1,2], Maureen Auro[1], C. Ashley Norris[4], and Gerhard Wörner[5]

[1]NIRVANA Laboratories, Woods Hole Oceanographic Institution, Woods Hole, MA, USA, [2]Department of Geology and Geophysics, Woods Hole Oceanographic Institution, Woods Hole, MA, USA, [3]University of Science and Technology of China, Hefei, China, [4]Department of Earth Sciences, University of Oxford, Oxford, UK, [5]Department of Earth Sciences, University of Göttingen, Göttingen, Germany

Abstract Thallium (Tl) isotope ratios are an emerging tool that can be used to trace crustal recycling processes in arc lavas and ocean island basalts (OIBs). Thallium is a highly volatile metal that is enriched in volcanic fumaroles, but it is unknown whether degassing of Tl from subaerial lavas has a significant effect on their residual Tl isotope compositions. Here, we present Tl isotope and concentration data from degassing experiments that are best explained by Rayleigh kinetic isotope fractionation during Tl loss. Our data closely follow predicted isotope fractionation models in which TlCl is the primary degassed species and where Tl loss is controlled by diffusion and natural convection, consistent with the slow gas advection velocity utilized during our experiments. We calculate that degassing into air should be associated with a net Tl isotope fractionation factor of $\alpha_{net} = 0.99969$ for diffusion and natural gas convection (low gas velocities) and $\alpha_{net} = 0.99955$ for diffusion and forced gas convection (high gas velocities). We also show that lavas from three volcanoes in the Kamchatka arc exhibit Tl isotope and concentration patterns that plot in between the two different gas convection regimes, implying that degassing played an important role in controlling the observed Tl isotope compositions in these three volcanoes. Literature inspection of Tl isotope data for subaerial lavas reveals that the majority of these appear only minorly affected by degassing, although a few samples from both OIBs and arc volcanoes can be identified that likely experienced some Tl degassing.

Plain Language Summary Volcanic degassing is an important process for understanding emissions to the atmosphere of greenhouse gasses and toxic metals. Thallium (Tl) is a toxic metal that is highly volatile, which in recent years has been developed as a stable isotope system that can be applied to understand the transfer of material from the Earth surface to the deep mantle via measurements of volcanic lavas. However, degassing of Tl from volcanic lavas could potentially alter the isotope ratio of the residual lava and, thus, render applications of Tl isotopes in lavas difficult to relate to deep Earth material transfer. Here, we perform the first study of Tl isotopes in degassing experiments. These reveal that Tl isotope ratios progressively become enriched in the heavy isotope with loss of Tl. We also show that natural lavas from Kamchatka follow similar Tl depletion and isotope enrichment patterns as our experiments, which for the first time demonstrates that degassing in nature is associated with diffusion-controlled loss of the light Tl isotope.

1. Introduction

Recycling of oceanic crust and sediments into the mantle at subduction zones is one of the most important processes occurring in the solid Earth. It controls the vast majority of mass transfer between the surface and deep Earth including water and other volatiles as well as radiogenic heat-producing elements like K, Th, and U. Thus, crustal recycling is the primary determinant of the viscosity and heat budget of the Earth's mantle. In addition, these recycled crustal reservoirs are thought to give rise to mantle plumes that are expressed at the Earth's surface as ocean island basalts (OIBs) or large igneous provinces (LIPs) (e.g., Hofmann & White, 1982). Much research has focused on understanding the physical and chemical consequences of crustal recycling, both those occurring during subduction itself and those associated with

mantle plume activity (e.g., Hofmann, 1997; Ryan & Chauvel, 2014). However, the time scales, mixing relationships, and connection between subduction and mantle plumes remain topics of debate (e.g., Cabral et al., 2013; Sobolev et al., 2019). New stable isotope ratio tools have emerged in the last two decades that promise to place new constraints on these aspects of crustal recycling (e.g., Andersen et al., 2015; Foden et al., 2018; Freymuth et al., 2015; Nielsen, Rehkämper, Norman, et al., 2006; Nielsen et al., 2018), which have the potential to elucidate the underlying reasons for the chemical and isotopic differences observed between different OIBs and LIPs.

Thallium (Tl) isotope compositions ($\varepsilon^{205}\text{Tl} = 10{,}000 \times ({}^{205}\text{Tl}/{}^{203}\text{Tl}_{\text{sample}} - {}^{205}\text{Tl}/{}^{203}\text{Tl}_{\text{SRM 997}})/({}^{205}\text{Tl}/{}^{203}\text{Tl}_{\text{SRM 997}})$ where SRM 997 is the NIST SRM 997 Tl isotopic standard) are emerging as a powerful tracer of crustal recycling processes due to the stark differences observed between Tl isotope compositions in marine sediments, altered oceanic crust, and the mantle (Nielsen, Rehkämper, Norman, et al., 2006; Nielsen, Rehkämper, Teagle, et al., 2006; Nielsen, Rehkämper, et al., 2017; Rehkämper et al., 2002, 2004). In addition, Tl concentrations in recycled crustal materials are several orders of magnitude higher than the ambient mantle, which provides strong mixing leverage when mixing between crustal and mantle components takes place. These characteristics have led to Tl isotopes finding utility in both establishing budgets of sediment cycling in subduction zones (Nielsen et al., 2016; Nielsen, Prytulak, et al., 2017; Prytulak et al., 2013; Shu et al., 2017) as well as identifying specific ocean crust and sediment components associated with deeply subducted materials and plumes (Blusztajn et al., 2018; Nielsen, Rehkämper, Norman, et al., 2006; Nielsen et al., 2007; Shu et al., 2019).

Several aspects complicate the interpretation of Tl isotope variation in lavas from arcs and OIBs. First, assimilation of modern crustal material during magma ascent could produce false positives for the presence of recycled crustal components (both sediments and oceanic crust), although the differences in radiogenic isotopic trace element compositions between OIBs, arc lavas, and possible assimilates allow reasonably robust tests of such processes for most samples (Blusztajn et al., 2018; Nielsen, Rehkämper, Norman, et al., 2006). Second, weathering processes like partial dissolution and secondary mineral precipitation can also affect both Tl concentrations and isotopic compositions (Howarth et al., 2018; Nielsen et al., 2016; Nielsen, Prytulak, et al., 2017). These processes are, however, readily identified with other physical and geochemical indices, such as thin-section inspections, loss on ignition, chemical index of alteration, radiogenic isotopes (e.g., $^{87}\text{Sr}/^{86}\text{Sr}$), and trace element ratios (e.g., Rb/Cs).

Finally, Tl is a highly volatile metal and, therefore, loss of Tl during magma degassing is possible. This process can affect both concentrations and isotope compositions of erupted lavas if Tl loss is associated with kinetic isotope fractionation whereby the light isotope (^{203} Tl) is lost preferentially to the heavy isotope (^{205} Tl), thus resulting in progressively heavier Tl isotope compositions in the residual lava. Although stable isotope fractionation of Tl can also be produced by equilibrium fractionation processes that are both mass-dependent and mass-independent (Moynier et al., 2013; Schauble, 2007), these are generally very minor in high-temperature processes (Nielsen et al., 2016; Prytulak et al., 2017) and are unlikely to be associated with volcanic degassing. Data from volcanic fumaroles have shown large ranges in Tl isotope compositions (Baker et al., 2009) that are on the order of the variations observed in both sediments and altered oceanic crust, suggesting that Tl isotope fractionation does take place during degassing and that Tl isotope variations associated with these kinetic effects (as opposed to the equilibrium effects mentioned above) could be significant. However, on average, these fumaroles appeared indistinguishable from basaltic lavas (although the lavas the fumaroles were degassed from were not measured), suggesting that, overall, degassing is typically not associated with net Tl isotope fractionation. Nevertheless, in several studies of arc lavas and OIBs samples have been identified where degassing processes were suspected to have significantly influenced Tl concentrations and isotope compositions, prompting these to be discounted from interpretations relating to crustal recycling (Nielsen, Prytulak, et al., 2017). However, it is still an open question whether Tl isotope fractionation by degassing occurs and, if so, what the magnitude of the associated isotopic fractionation is.

Here, we present Tl concentration and isotope data from degassing experiments that reveal significant isotopic fractionation as a function of Tl loss. We also present data for a set of basaltic lavas from the Kamchatka arc to test the potential effects of lava degassing in natural samples. These samples were selected because a significant sediment contribution to their mantle wedge magma source has been excluded in previous studies (Churikova et al., 2001, 2007; Dorendorf, Churikova, et al., 2000; Dorendorf, Wiechert, et al., 2000;

Table 2
Tl Isotope Composition and Concentrations for Degassing Experiments

Sample	ε^{205} Tl	Tl (μg/g)	Cr (μg/g)[a]	CO/CO_2	Gas molar mass (g/mol)
Starting material	3.5	403	601		
FO 08	6.8	190	607	0.044	43.3
FO 14	8.1	152	713	0.435	39.2
FO 18	10.8	44	595	4.348	31.0
FO 19	12.1	37	701	43.444	28.4

[a]Cr concentrations from Norris and Wood (2017).

Huang et al., 2018; Liu et al., 2020; Münker et al., 2004). These Kamchatka lavas show Tl concentration and isotope patterns for individual volcanoes that are identical to those produced by the degassing experiments. Moreover, the total Tl isotope variation is as large or larger than that associated with crustal recycling. Our data, therefore, imply that degassing can be an important process in modifying Tl isotope compositions of mantle-derived lavas that erupt subaerially.

2. Samples and Methods

2.1. Experimental Procedures

The experiments used a novel one-atmosphere gas-mixing furnace in which the sample can be continuously stirred at high temperature under controlled oxygen fugacity (Norris & Wood, 2017). The crucible and stirrer mechanism were made of high-purity nickel. The total furnace tube length is 720 mm and its internal diameter 45 mm. The ends are sealed with O-rings and metal end-caps and the latter cooled with recirculating chilled water. The starting material was a natural basalt from the Reykjanes Peninsula crushed and ground using an agate disc mill and doped with 300–500 μg g^{-1} of a number of trace elements (Ag, Bi, Cd, Cr, Cu, Ga, Ge, In, Pb, Sb, Sn, Tl, and Zn) each added as reagent-grade oxide. The experimental charges used here are the same as those produced previously (Norris & Wood, 2017).

For each experiment, 3 g of material was weighed out, pressed into a 12-mm diameter pellet and placed inside the 18-mm internal diameter crucible. The crucible was introduced into the preheated furnace from below, standing on an alumina pedestal. The crucible took about 2 min to reach melting temperature, after which the stirrer was introduced from above, inserted ∼8 mm into the melt and the furnace sealed. Volatile loss experiments (Table 2) were performed for 60 min at 1,300°C and a range of log fO_2 values from −7 (experiment number FO08) to −13 (experiment number FO19). The oxygen fugacities of the experiments were controlled using CO/CO_2 gas mixtures of known ratio and checked using a solid zirconia potentiometric oxygen sensor. The control gas flow rate through the furnace was equivalent to a linear velocity of 0.1 cm/s and the sample melt was stirred at 30 rpm. At the end of the experiment, a trapdoor in the bottom of the furnace was opened, allowing the pedestal and assembly to fall into a water bath.

The Ni crucible was mounted in epoxy and sliced in half with a diamond wafering saw to expose the clear quenched glass sample. One half of the capsule was polished and glass for isotopic analysis dug out using a diamond dentist's drill-bit.

2.2. Kamchatka Lavas

Subduction-related volcanism in Kamchatka occurs in three trench-parallel volcanic belts: the Eastern Volcanic Front (EVF) is located closest to the trench about 100 km above the subducting Pacific plate (Gorbatov et al., 1997), the Central Kamchatka Depression (CKD), and the Sredinny Ridge back-arc region (SR) (Churikova et al., 2001). We present new Tl isotope and concentration analyses on a series of Holocene low to medium K calc-alkaline lavas from three volcanoes in the Kamchatka arc: Gamchen and Komarov from the EVF, and Bakening at the southern extension of the CKD located about 200 km above the subducting slab (Gorbatov et al., 1997). Samples were selected to be visually perfectly fresh and to cover the entire compositional range documented by previously analyzed major and trace element compositions and radiogenic isotope measurements (Churikova et al., 2001; Dorendorf, Churikova, et al., 2000; Dorendorf, Wiechert, et al., 2000). Bakening rocks (total of 13) are exclusively basalts with high MgO = 7.8%–9.8% and relatively minor amounts of fractional olivine and pyroxene crystallization (Figure 1). Samples from Gamchen (total of 7) range from SiO_2 = 49.8%–55.4% and MgO = 3.0%–6.2%, which can be accounted for mainly by fractional crystallization of olivine and pyroxene from a basaltic parental magma (Figure 1). Here, we use plots of MgO versus Co and CaO versus Sc to qualitatively assess crystallization of olivine and clinopyroxene, respectively. These elements are used because Mg and Ca are primary constituents of olivine and clinopyroxene, respectively. At the same time, Co is compatible in olivine and incompatible in clinopyroxene, while Sc is incompatible in olivine and compatible in clinopyroxene (Le Roux et al., 2011). Finally, lavas

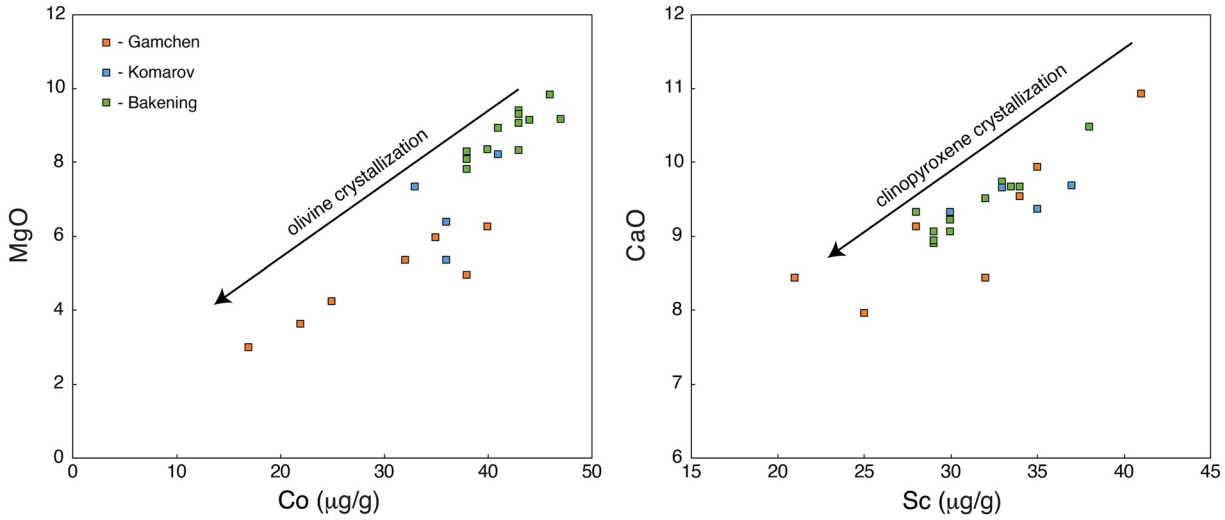

Figure 1. Major and trace element plots for lavas from Gamchen, Bakening, and Komarov volcanoes in Kamchatka. Arrows denote generic direction of chemical evolution expected for olivine and clinopyroxene fractional crystallization.

from Komarov (total of 4) have ranges of SiO_2 = 51.7%–53.7% and MgO = 5.4%–8.2% that have a poorer fit with fractional crystallization from a single starting composition, perhaps suggesting the influence of other mineral phases or multiple magmas (Figure 1). However, in general, the compositional variations in the lavas erupted from these centers are relatively small and can be accounted for mainly by fractional crystallization, which is also consistent with all Kamchatka lavas being erupted during Holocene times over a relatively short time span (Ponomareva et al., 2007). Radiogenic Sr isotope compositions are relatively uniform for samples from a particular volcano and are also close to MORB values (Churikova et al., 2001; Dorendorf, Churikova, et al., 2000; Dorendorf, Wiechert, et al., 2000). These observations together suggest that the magma source was relatively uniform. Fluid-mobile elements, however, show large enrichments and are more variable as expressed in high and variable ratios of B/La, Ba/Nb (Churikova et al., 2007) and As/Ce or Sb/Ce (Liu et al., 2020).

2.3. Thallium Isotope and Concentration Measurements

We used aliquots of previously investigated sample powders of the Kamchatka lavas or small glass fragments (~10 mg) from the experimental charges (Norris & Wood, 2017). All samples were dissolved in a 5:1 mixture of concentrated distilled HNO_3 and HF on a hotplate for 24 h. They were then dried and fluxed several times using a 1:1 mixture of concentrated distilled HNO_3 and HCl until the fluorides, which formed in the first step, were completely dissolved. Following this, samples were dried again on a hotplate and dissolved in 1 M hydrochloric acid for ion exchange chromatographic separation of Tl. Thallium was separated from the matrix of samples in the NIRVANA (Non-traditional Isotope Research for Various Advanced Novel Applications) clean lab at Woods Hole Oceanographic Institution (WHOI) using published ion-exchange chromatographic methods (Nielsen et al., 2004; Nielsen & Rehkämper, 2011; Rehkämper & Halliday, 1999). Total procedural blanks including sample dissolution and column chemistry for Tl were determined for every set of samples processed through the column chemistry and were always <2 pg, which is significantly less than the minimum amounts of Tl processed (~1.5 ng) and, therefore, negligible.

The Tl isotope compositions were analyzed on a Thermo Finnigan Neptune multiple collector inductively coupled plasma mass spectrometer (MC-ICPMS), located in the WHOI Plasma Facility. External correction for mass discrimination to NIST-SRM 981 Pb and standard-sample bracketing of the NIST-SRM 997 Tl standard were applied for analysis of Tl isotope compositions (Nielsen et al., 2004; Nielsen & Rehkämper, 2011; Rehkämper & Halliday, 1999). Tl concentrations were determined by monitoring the ^{205} Tl intensity during the isotopic measurements, because the column chemistry procedure returns quantitative Tl yields (Nielsen et al., 2004; Nielsen & Rehkämper, 2011; Rehkämper & Halliday, 1999). The measured

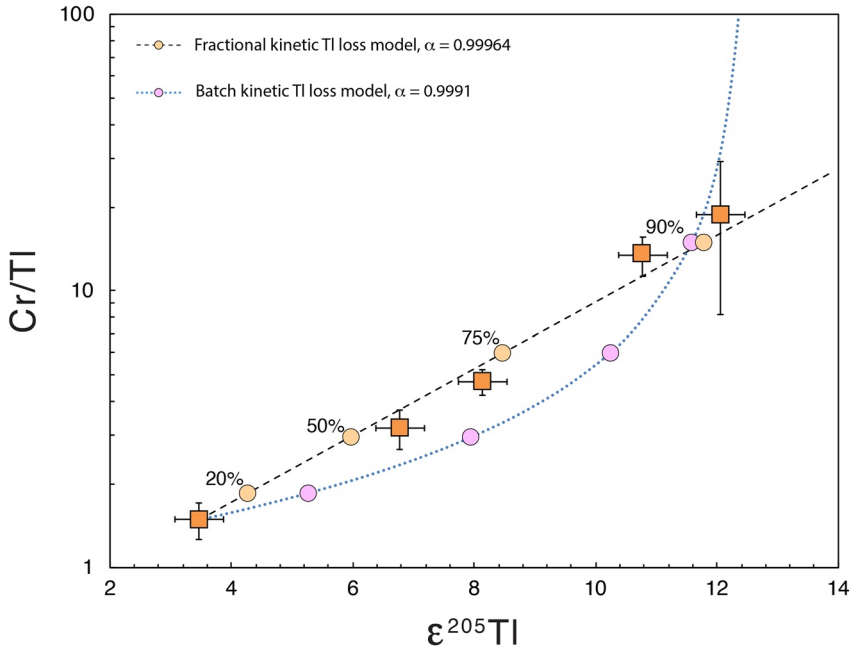

Figure 2. Thallium isotope compositions plotted against Cr/Tl ratios for degassing experiments. Also shown are two models in which the starting material is either degassed via fractional loss or batch loss mechanisms. Chromium is assumed refractory in the experiments such that only Tl loss affects the Cr/Tl ratio.

^{205} Tl/^{208}Pb ratios were converted directly into Tl concentrations by adding a known quantity of NIST-SRM 981 Pb to each sample after separation of Tl (Nielsen et al., 2015). Throughout the course of this study, the USGS basalt powder BHVO-1 was also processed together with sample unknowns to monitor data quality. These analyses, which have been presented in previous manuscripts, displayed Tl isotopic compositions consistent with literature values of ε^{205} Tl = −3.6 ± 0.4 (2sd, n = 43) (Shu et al., 2017, 2019). Similarly, Tl concentration measurements of BHVO-1 yielded values (40 ± 5 ng/g; 2sd) within the error of previous study (Makishima & Nakamura, 2006; Nielsen et al., 2015; Prytulak et al., 2013). As in previous studies, we use these uncertainties throughout this manuscript as our best estimates of the total external error on individual Tl isotope and concentration measurements.

Concentrations of Tl and Cr in the experimental charges were also measured by laser ablation ICPMS (Norris & Wood, 2017) and the reported Tl concentrations are averages of the values determined via the two techniques.

3. Results

Thallium concentrations and isotope compositions for degassing experiments and the starting material are shown in Table 2 and plotted in Figure 2. Here, it can be seen that the starting material had the highest Tl concentration and lightest isotope composition, with progressively lower Tl concentrations and heavier isotope compositions for the degassing experiments that reveal between 60% and 90% Tl loss and a change of almost 9 ε^{205}Tl-units relative to the starting material (Figure 2).

Data for lavas from Gamchen, Komarov, and Bakening are shown in Table 1. These samples also show a general tendency of lower Tl concentrations being associated with progressively heavier Tl isotope compositions when considering the volcanoes individually. Normalization of Tl abundances to Ce, which has a similar bulk partition coefficient to Tl (Nielsen et al., 2014), reveals systematic enrichments in heavy Tl isotopes as Ce/Tl ratios increase (Figure 3).

Table 1
Geochemical Data for Lavas From Gamchen, Komarov, and Bakening Volcanoes

Sample	SiO_2	TiO_2	Al_2O_3	Fe_2O_3	FeO	MnO	MgO	CaO	Na_2O	K_2O	P_2O_5	LOI	Sc	Co	Ce	Tl	ε^{205} Tl
Gamchen volcano																	
GAM-96-14	55.8	0.86	18.5	3.38	5.39	0.18	3.62	7.96	3.26	0.33	0.13	0.46	25	22	9.4	0.0096	13.5
GAM-96-16	54.9	0.80	18.1	2.59	5.79	0.17	4.23	8.44	2.86	0.85	0.11	0.34	32	25	nd	0.0517	−0.3
GAM-96-28	49.8	0.83	17.9	2.59	7.96	0.20	6.24	10.93	2.37	0.66	0.13	0.21	41	40	13.1	0.0259	1.2
GAM-96-07	51.6	0.85	18.6	3.43	5.73	0.18	5.35	9.12	2.72	0.49	0.12	1.58	28	32	11.5	0.0384	−0.9
GAM-96-12	54.7	0.80	19.8	2.30	4.67	0.14	2.98	8.44	3.18	0.68	0.12	0.46	21	17	nd	0.0517	0.6
GAM-96-22	52.8	0.80	17.2	2.49	6.88	0.19	5.95	9.54	2.78	0.54	0.12	0.60	34	35	12.7	0.0477	−2.1
GAM-96-26	50.6	1.00	18.5	2.87	8.48	0.20	4.94	9.93	2.60	0.61	0.11	0.46	35	38	10.9	0.0455	−1.5
Komarov volcano																	
KOM-96-02/2	53.7	0.75	16.0	1.86	6.48	0.17	7.33	9.36	2.55	0.80	0.12	0.70	35	33	9.8	0.0790	−2.5
KOM-96-06	51.7	0.83	16.3	2.03	7.47	0.18	8.20	9.68	2.41	0.68	0.11	0.56	37	41	9.9	0.0523	−0.6
KOM-96-01	52.6	0.84	17.2	2.20	7.01	0.18	6.39	9.66	2.58	0.79	0.13	0.41	33	36	11.8	0.0590	−0.8
KOM-96-14	53.5	0.81	17.8	3.19	6.24	0.18	5.36	9.33	2.83	0.56	0.12	0.36	30	36	10.4	0.0373	0.7
Bakening volcano																	
BAK-95-17	51.2	1.15	16.3	2.01	6.52	0.16	8.29	8.90	3.38	1.01	0.29	0.60	29	38	26.7	0.0753	−0.7
BAK-95-24	49.7	1.03	16.2	2.46	6.91	0.17	9.83	9.67	2.87	0.70	0.21	0.60	34	46	19.4	0.0397	1.6
BAK-95-31	50.3	1.09	16.1	2.24	6.89	0.17	9.15	9.32	3.21	0.95	0.26	0.27	30	44	24.7	0.0627	3.4
BAK-95-14	50.3	0.99	16.4	2.18	7.02	0.18	8.92	9.74	3.00	0.68	0.23	0.49	33	41	21.5	0.0484	0.4
BAK-95-15	50.1	0.96	16.8	2.60	6.73	0.19	8.33	9.51	3.00	0.77	0.26	0.51	32	40	23.2	0.0403	1.2
BAK-95-30	50.5	1.08	16.3	2.58	6.56	0.17	9.05	9.22	3.16	0.94	0.26	0.32	30	43	23.4	0.0648	0.5
BAK-95-33	51.3	1.03	16.8	2.35	6.56	0.17	8.32	9.06	3.14	0.92	0.23	0.43	29	43	23.0	0.0582	0.9
BAK-95-34	51.2	1.04	16.9	2.08	6.70	0.17	7.80	8.94	3.18	0.91	0.23	0.47	29	38	22.7	0.0832	−0.4
BAK-96-04	48.8	1.13	17.3	2.68	7.09	0.17	8.09	10.5	2.83	0.70	0.17	0.25	38	38	18.2	0.0088	6.7
O-95-26	50.4	1.10	16.3	2.53	6.42	0.15	9.40	9.06	3.22	0.90	0.28	0.23	30	43	23.8	0.0283	4.7
23	49.7	1.16	15.8	2.81	6.79	0.16	9.30	9.33	3.05	1.35	0.39	0.14	28	43	30.8	0.0432	3.9
23/1	49.8	1.15	15.8	4.30	5.35	0.16	9.17	9.33	3.08	1.36	0.39	0.25	30	47	31.1	0.0119	8.3

Note. Major element oxides and loss on ignition (LOI) in weight %; Trace elements in μg/g. Major elements, LOI, Sc, Co, and Ce from Dorendorf, Churikova, et al. (2000), Dorendorf, Wiechert, et al. (2000), and Churikova et al. (2001), Tl concentrations and isotope compositions from this study.
Abbreviations: LOI, loss on ignition; nd, not determined.

4. Discussion

4.1. Experimental Tl Isotope Fractionation

Generally, the pattern of heavier Tl isotope compositions as a function of Tl depletion (Table 2) is consistent with kinetic isotope fractionation of Tl during degassing. To correct for potential mass loss from the entire experiment we normalize the Tl abundances to the relatively refractory element, Cr (Figure 2). For consistency with the natural lava data, it would have been ideal to normalize the Tl abundances to Ce for the experimental glasses as well. However, this element was not determined for the experimental products and, in any case, degassing of Cr was not sufficient to cause any detectable loss (Table 2).

We can reproduce the coupled Tl loss and kinetic isotope fractionation through an open-system fractional Rayleigh model:

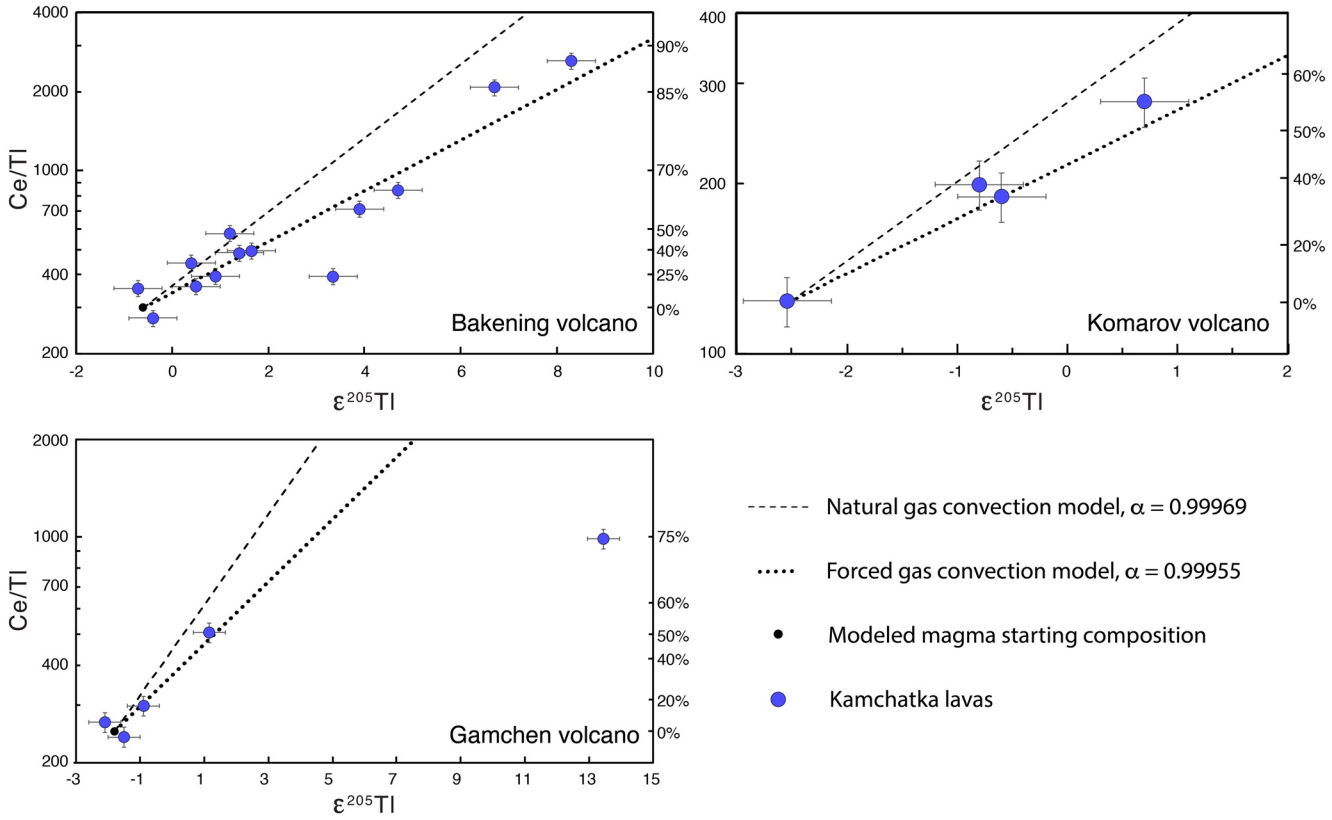

Figure 3. Thallium isotope compositions plotted against Ce/Tl ratios for lavas from Bakening, Komarov, and Gamchen volcanoes. Plotted are also the two different kinetic degassing models for natural and forced gas convection (see text for details). The starting composition of each volcano was estimated based on the least degassed samples. The secondary axis shows Tl loss in percent relative to the modeled starting composition.

$$R_t = R_0 \times \left(\frac{C_t}{C_0}\right)^{(\alpha-1)} \quad \text{(eq 1)}$$

where R_t and R_0 are the Tl isotope compositions of the residual degassed experimental products at time t and the starting material, respectively; C_t and C_0 are the Tl concentrations of the residual degassed experiment at time t and the starting material, respectively; and α is the constant isotope fractionation factor between fractional volume of gas and its residual at any given point in time, $R_{gas}/R_{residual}$. This equation applies when the evaporating source is changing but of uniform composition at all times. Alternatively, we can construct a closed-system batch model where the entire amount of degassed Tl is equilibrated with the residual melt before being released according to the equation:

$$R_t = R_0 \times \frac{1}{\frac{C_t}{C_0} + \alpha\left(1 - \frac{C_t}{C_0}\right)} \quad \text{(eq 2)}$$

It should, however, be noted that the experimental conditions, where gas was continuously removed from the solid residue by advection, make this latter model relatively improbable. The average fractionation factors that best fit the experimental data are $\alpha_{frac} = 0.99964$ for the fractional model and $\alpha_{batch} = 0.9991$ for the batch model (Figure 2). However, the fractional model provides a better overall fit to the data, which is also consistent with the experimental conditions in the 1 atm furnace that allowed free degassing of volatile elements into a gas that was flowing slowly across the sample surface.

Recent study has provided a theoretical basis for degassing-induced stable isotope fractionation (Richter et al., 2002, 2011; Sossi et al., 2020; Young et al., 2019). This study has resulted in predictions of net fractionation factors at atmospheric pressure for the cases of control by diffusion into a gas that is under a forced convection regime (Young et al., 2019) and diffusion into a gas under a natural convection regime (Sossi et al., 2020). The principal difference between these two approaches is that the gas velocity is significantly lower for the natural convection case (all else being equal), which results in the mass transfer coefficient (k_c) taking two different forms (Chilton & Colburn, 1934; Frössling, 1938; Sossi et al., 2020). Both approaches predict that net isotopic fractionation (α_{net}) between two isotope species with masses m_i and m_j in terrestrial lavas primarily depends on the reduced masses μ_{ik} and μ_{jk} as follows:

$$\alpha_{net} = \left(\frac{\mu_{jk}}{\mu_{jk}}\right)^{\beta} \quad \text{(eq 3)}$$

where μ_{ik} is the reduced mass $m_i m_k/(m_i + m_k)$ that also includes the molar mass of the ambient gas phase m_k and β of either 1/2 (in the case of diffusion with forced convection; Young et al., 2019) or 1/3 (in the case of diffusion with natural convection; Sossi et al., 2020). These exponents are a direct consequence of the two expressions for k_c under the two gas convection regimes.

In the following, we discuss the likely mass of the isotopic species (m_i and m_j) of Tl that need to be considered in the experiments we conducted. Previous empirical study on lavas has suggested that Tl degasses as the TlCl species (Churakov et al., 2000), although thermodynamic considerations suggest that reduced Tl^0 gas (Barin et al., 1989) may also be important. Recent study on the relationship between the Cl contents of basalts and their Cl_2 fugacities (Thomas & Wood, 2021) can be used to calculate the ratio of TlCl to Tl^0 during equilibrium degassing. Although we do not know the exact Cl content of the Icelandic basalt used for the experiments, the average Cl content of 64 Icelandic basalts in the GEOROC database is 550 μg/g (1σ = 190 μg/g). We used this concentration together with the relationship between Cl content and Cl_2 fugacity from Thomas and Wood (2021) and thermodynamic data on the gas species (Barin et al., 1989) to calculate the ratio of TlCl to Tl^0 at the oxygen fugacities of the experiments. At 1,300°C we obtain values of between 6 (at $fO_2 = 10^{-13}$) and 180 (at $fO_2 = 10^{-7}$) for the TlCl:Tl^0 ratio in our experiments. Even if the true Cl concentration is 1 standard deviation (190 μg/g) lower than assumed, the TlCl:Tl^0 ratios would only drop to 4 (at $fO_2 = 10^{-13}$) and 115 (at $fO_2 = 10^{-7}$). TlCl should therefore dominate in our experiments, but Tl^0 may be significant under the most reducing conditions. For these reasons, oxygen fugacity is not expected to impart any direct control on the isotope fractionation factors observed in our experiments. Furthermore, it has been argued based on theoretical considerations that, apart from possible changes in speciation and the molar mass of ambient gas, oxygen fugacity does not control kinetic isotope fractionation during degassing because k_c is largely independent of fO_2 (Sossi et al., 2020).

Due to the different masses of Tl^0 and TlCl, it is important to consider both species when calculating theoretical Tl isotope fractionation factors. In addition, the molar mass, m_k, of the ambient gas has a large effect on α_{net} (Equation 3), which is important to consider here because our experiments were conducted with variable mixtures of CO and CO_2 (Norris & Wood, 2017), which leads to different molar masses for the ambient gas in each experiment (Table 2). Although all the experiments fit a general fractionation trend relatively well (Figure 2) it can be seen that experiments FO 8 and FO 14 plot slightly below the best fit line, whereas FO 18 and FO 19 plot slightly above. This is well explained by the variations in molar mass of the gas in the experiments (Equation 3, Table 2).

Here, we calculate predicted fractionation factors for Tl^0 and TlCl species using diffusion in both forced and natural gas convection cases (Table 3). The comparison between predicted and measured Tl isotope fractionation factors reveals a strong fit between TlCl degassing in a system controlled primarily by diffusion and natural gas convection (Figure 4). Even though no Cl was added to the experiments, it appears that background abundances of Cl were sufficient to dominate the Tl speciation during degassing, even for the most reduced of our experiments, which, as outlined above, is consistent with the average literature Cl abundances for Icelandic basalts. Our calculations also imply that the natural gas convection formulation of kinetic isotope fractionation during degassing more closely approximates the behavior of Tl and its isotopes during degassing in our experiments than the forced gas convection-diffusion model (Figure 4). This result

Table 3
Calculated and Measured Tl Isotope Fractionation Factors for Degassing Experiments

Experiment	Tl loss (%)[a]	α_{net} Tl^0, $\beta = 0.33$	α_{net} TlCl, $\beta = 0.33$.	α_{net} Tl^0, $\beta = 0.5$	α_{net} TlCl, $\beta = 0.5$	α_{net} measured	Error[b]
FO 08	53.4	0.99943	0.99957	0.99914	0.99936	0.99957	0.00007
FO 14	68.3	0.99947	0.99961	0.99921	0.99941	0.99959	0.00004
FO 18	88.9	0.99957	0.99968	0.99935	0.99952	0.99967	0.00003
FO 19	92.1	0.99960	0.99970	0.99940	0.99956	0.99966	0.00005

[a]Tl loss is calculated based on Cr/Tl ratios in experiments relative to the starting material. [b]Errors propagated based on the uncertainties of the Tl concentrations and isotope compositions.

is consistent with the low velocity of the advective gas transport (0.1 cm/s) that was part of our experimental setup (Norris & Wood, 2017).

Although our experimental results fit exceptionally well with the theoretical formulation of TlCl degassing based on the natural gas convection case (Sossi et al., 2020), there are several reasons why natural samples might not adhere exclusively to this formulation. First, both the natural and forced gas cases require the solid medium to be well mixed during degassing, which is more difficult to achieve for more viscous melts. Second, the speciation of Tl in a melt could vary as a function of the oxygen fugacity in concert with the concentrations of Cl and other ligand-producing species such as S that might affect the degassed Tl species (Johnson & Canil, 2011). Finally, the dominant mode of degassing in nature is likely to vary and may not always correspond most closely with the natural gas convection formulation.

In the following, we examine Tl isotope and concentration patterns from three Kamchatka arc volcanoes to compare our experimental results with natural samples.

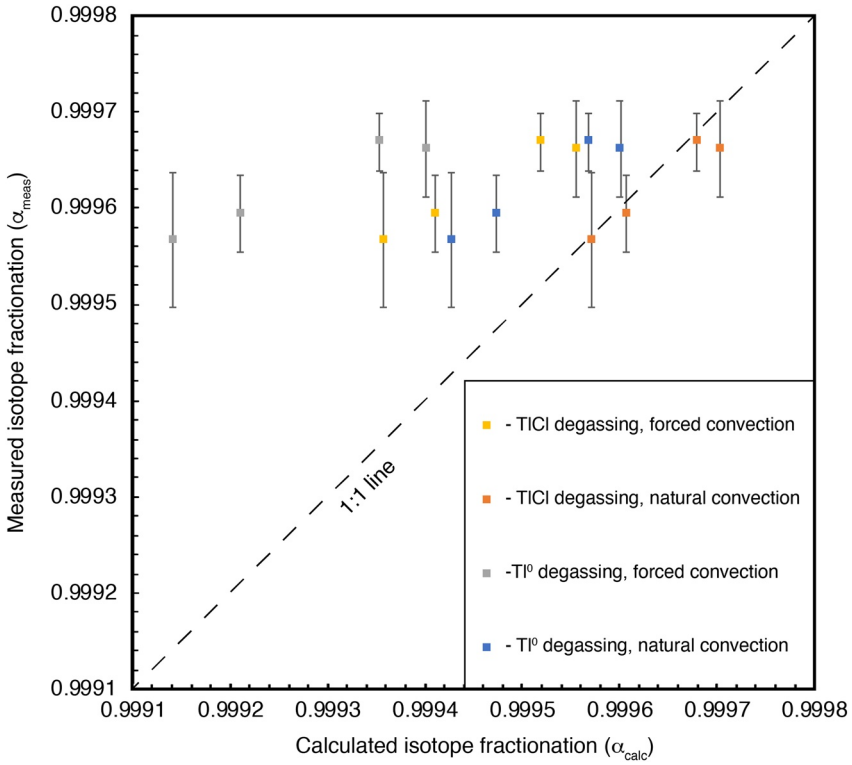

Figure 4. Measured and calculated Tl isotope fractionation factors for our four degassing experiments. Data are listed in Table 3. The calculated fractionation factors were computed using Equation 3 with an exponent of $\beta = 0.5$ for forced gas convection and $\beta = 0.33$ for natural gas convection.

4.2. Natural Degassing From Kamchatka Volcanoes

Sample suites from Gamchen, Komarov, and Bakening volcanoes also show increasing ε^{205}Tl-values as a function of increasing Ce/Tl ratios (Figure 3). Because Tl concentrations may also be affected by fractional crystallization, variations in the Tl budget of erupted lavas are best monitored via normalization to Ce, which exhibits the same bulk partition coefficient as Tl (Nielsen et al., 2014). It is well known that Tl in arc lavas is sourced primarily from the slab (Nielsen, Prytulak, et al., 2017; Noll et al., 1996) and that these slab sources can exhibit large Tl isotope variations (Nielsen et al., 2016; Nielsen, Prytulak, et al., 2017; Prytulak et al., 2013; Shu et al., 2017). The only known slab source that consistently exhibits heavy Tl isotope compositions is pelagic clays (Nielsen et al., 2016; Rehkämper et al., 2004) because they are enriched in Mn oxides that absorb large quantities of isotopically heavy Tl (Nielsen et al., 2013). Hence, the heavy Tl isotope compositions in the Kamchatka lavas could be consistent with the addition of variable amounts of pelagic sediment to the melting region. However, previous studies have concluded that sediments are essentially absent in the Kamchatka melting region (Churikova et al., 2001, 2007; Dorendorf, Churikova, et al., 2000; Dorendorf, Wiechert, et al., 2000; Huang et al., 2018; Liu et al., 2020; Münker et al., 2004) and pelagic clays are associated with Ce/Tl ratios as low as 20 (Nielsen et al., 2016; Nielsen, Prytulak, et al., 2017; Shu et al., 2017). Thus, the trend toward heavy isotope compositions with increasing Ce/Tl ratios in the Kamchatka lavas cannot be explained by variable slab inputs.

These trends can instead be compared with the expected values of α_{net} when degassing into air and diffusion under the forced and natural convection cases. Based on the calculated values for diffusion and convection in air it would be predicted that natural basaltic lavas should be associated with $\alpha_{net} = 0.99969$ for the case of slower (natural) gas convection and $\alpha_{net} = 0.99955$ for the case of forced gas convection. The data from the three volcanoes in the Kamchatka arc appear to plot in between the two degassing models, suggesting that natural systems experience different periods of degassing that are best approximated by both models.

However, as outlined in Section 4.1, the magnitude of α_{net} may vary for different magmatic systems, in particular for melts with low Cl contents (e.g., <100 μg/g) and high S contents that would potentially change the speciation of Tl in the melt, or high viscosities that would attenuate the magma homogeneity during degassing. Thus, both the mode of degassing and the composition and physical state of the melt may have an influence on α_{net}.

Given that basaltic and andesitic Kamchatka lavas on average contain similar amounts of Cl to average Icelandic basalts (Izbekov et al., 2004; Ponomareva et al., 2013; Tolstykh et al., 2012), speciation is unlikely to explain the apparent variations in α_{net}. We can speculate about how the mode of degassing may control whether the forced or natural convection models better describe natural data in general. As a reminder, natural convection applies generally to relatively low gas velocities, whereas forced convection applies to higher gas velocities. Degassing can take place at multiple different stages of the eruption process, from during magma storage in a shallow magma chamber, to effusive eruption via strombolian activity, and finally during viscous flow of lavas and even after arrest until final solidification. If we consider these potential degassing stages in terms of the forced and natural gas convection models, it appears most likely that the natural convection scenario would primarily apply to the magma storage stage and not to the latter stages of eruption. In addition, lava flows often rapidly evolve into relatively viscous liquids due to cooling, which would tend to attenuate sample homogenization during degassing and render both formulations inappropriate. Thus, degassing in the vent after shallow fragmentation during final ascent and in the eruption plume during strombolian activity might present the most likely case to produce significant degassing that is associated with kinetic isotope fractionation under forced gas convection conditions. This equally applies to both scoria and massive lava flow samples because even massive lava flows generally pass through a phase of strombolian fountaining before collecting into flows. Finally, closed-system batch loss (Equation 2) could also theoretically be possible if early stages of degassing occurred in a closed magma chamber at largely atmospheric pressure. However, this possibility seems very unlikely.

In the end, the dominant parameter (degassing mode, Tl speciation, physical state of magma during degassing) in controlling variations in α_{net} is hard to determine exactly for the samples investigated here because even samples from the same volcano could derive from different magma starting compositions. In this way, small amounts of heterogeneity in either Ce/Tl and/or ε^{205} Tl of the starting magma could account for some

of the variability in perceived α_{net}. However, without a doubt the vast majority of the Tl isotope variation observed for these three Kamchatka volcanoes is caused by kinetic isotope fractionation during degassing.

4.3. Comparison with Literature Data

There are a number of studies that have reported Tl isotope data for subaerial basaltic lavas (Blusztajn et al., 2018; Nielsen, Rehkämper, Norman, et al., 2006; Nielsen et al., 2007, 2016; Nielsen, Prytulak, et al., 2017; Prytulak et al., 2013; Shu et al., 2017), which could in principle all have been affected by degassing. Previous studies typically assessed influence from degassing based on Ce/Tl ratios in combination with anomalously heavy Tl isotope compositions, which frequently resulted in removal from consideration of samples suspected of degassing. The results presented here clearly justify this earlier conservative approach, but we can furthermore use the new quantitatively determined Tl isotope fractionation factor to investigate if there is any evidence that previous studies have overestimated or underestimated effects from degassing. The primary difficulty in making a robust assessment of degassing in samples from previous studies is that most only analyzed small sample sets (1–3) from individual volcanoes, which precludes construction of clear degassing trends like those observed here for Kamchatka volcanoes (Figure 3). However, upon further inspection of several previously published data sets from the Marianas, Ryukyu arc, Aleutian arc, and the Azores it is possible to discern small effects from degassing not previously recognized (Figure 5). These four data sets were each carefully evaluated for degassing and it was concluded that Tl isotope variation could not confidently be ascribed to such a process (Nielsen et al., 2007, 2016; Prytulak et al., 2013; Shu et al., 2017). However, for the samples highlighted in Figure 5, that originate from individual volcanoes or volcanic centers, relatively strong correlations between Ce/Tl ratios and Tl isotope compositions are evident that also plot close to the two predicted Tl degassing trends with $\alpha_{net} = 0.99969$ and $\alpha_{net} = 0.99955$ that we show the three Kamchatka volcanoes plot in between (Figure 3).

We, therefore, conclude that the heaviest Tl isotope compositions in Azores and Mariana lavas likely were produced by degassing, which significantly attenuates the overall variation in these two locations. These samples were already flagged as anomalous relative to the remainder of samples analyzed in those two studies (Nielsen et al., 2007; Prytulak et al., 2013) and did not strongly affect their conclusions. Our new evidence for degassing simply underscores the relatively minor Tl isotope variations in these two locations, although both still consistently record Tl isotope values above the average depleted mantle (ε^{205} Tl $= -2 \pm 0.5$; Nielsen, Rehkämper, et al., 2017), which suggest influence from recycled pelagic sedimentary material.

Okmok volcano (Figure 5c) is situated in the Eastern Aleutians where lavas overwhelmingly exhibit Tl isotope compositions similar to average continental crust (ε^{205} Tl $= -2 \pm 0.5$ (Nielsen et al., 2005);), which was suggested to reflect the influence of subducted detrital material derived from the North American continent (Nielsen et al., 2016). Notably, the primary excursion from crustal-like Tl isotope compositions in the Eastern Aleutians were the heavier samples from Okmok, which now appear likely to reflect degassing. Thus, lavas from the Eastern Aleutians are even more invariant around the average crustal value, which reinforces the previous conclusion that Tl isotope systematics in this part of the Aleutian arc is dominated by subducted clastic sediments.

Finally, the degassed lavas from Hokusatsu (South Kyushu) (Figure 5d) also exhibit the heaviest Tl isotope compositions in the Northern portion of the Ryukyu arc (Shu et al., 2017). Similarly to the Aleutians, it was found that sediments subducted in this part of the arc strongly resemble average continental crust (Shu et al., 2017), with all lavas, except the two heavy samples here implied as degassed (Figure 5d), being indistinguishable from sediments measured outboard of this portion of the arc. Hence, accounting for the effect of degassing reduces the overall Tl isotope variation in Northern Ryukyu and strengthens the conclusions that were reached in the initial study.

It should be highlighted, however, that the majority of subaerial basaltic lavas appear to record either minor or no effects on Tl isotopes from degassing (Blusztajn et al., 2018; Nielsen, Rehkämper, Norman, et al., 2006; Nielsen et al., 2007, 2016; Nielsen, Prytulak, et al., 2017; Prytulak et al., 2013, 2017; Shu et al., 2017). This lack of significant Tl degassing was even evident in lavas covering large ranges of magmatic evolution (Nielsen et al., 2016; Prytulak et al., 2017), suggesting that time spent in a magma chamber before eruption is not the main factor controlling Tl degassing. As such, Tl isotope ratios should still be recognized as a

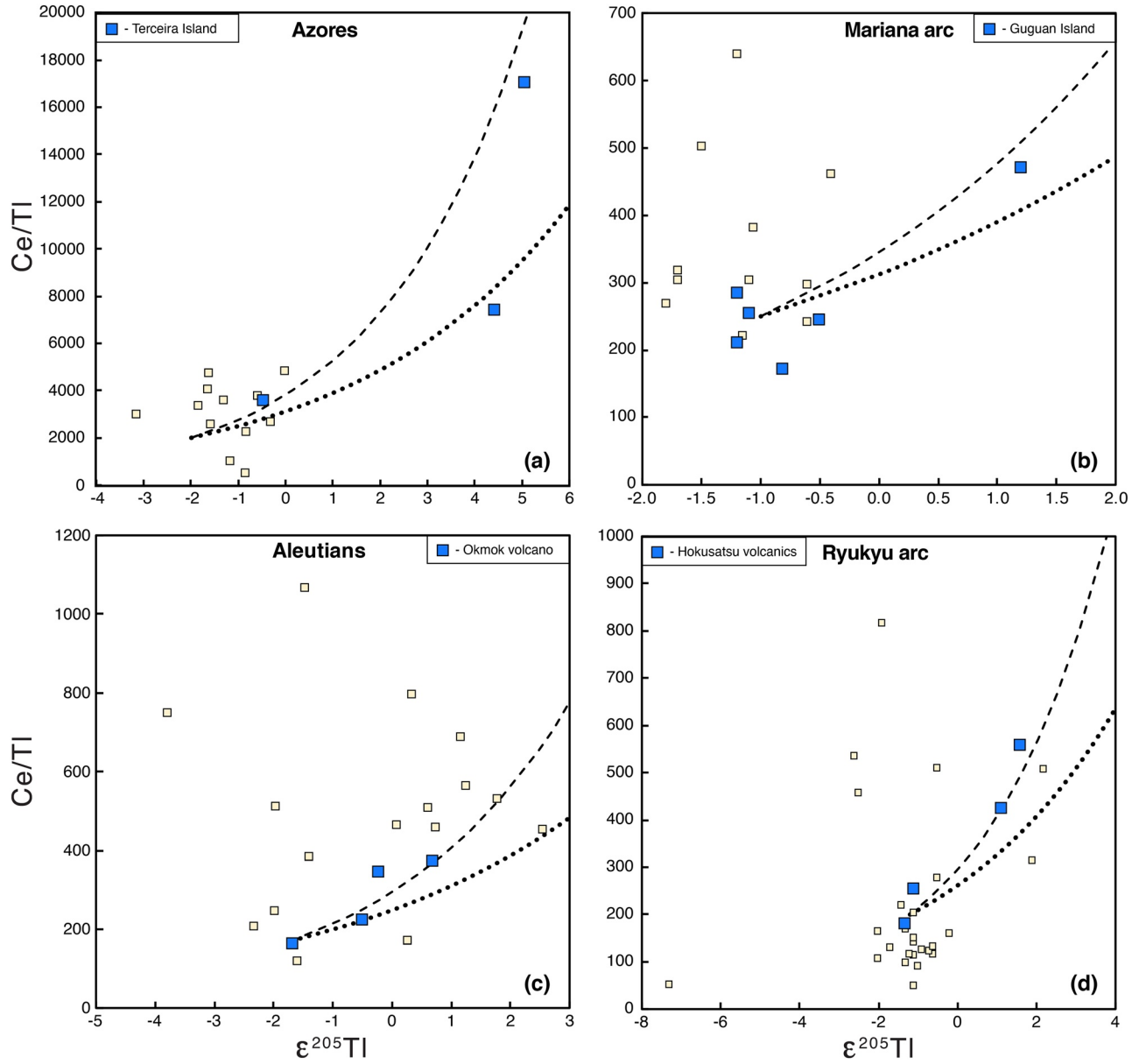

Figure 5. Thallium isotope compositions plotted against Ce/Tl ratios for lavas from Azores, Marianas, Aleutians, and Ryukyu arc (yellow squares). Blue squares denote samples from individual volcanoes or volcanic centers in which a degassing trend can be discerned. Shown are also the two Tl loss models with $\alpha_{net} = 0.99969$ (dashed line, natural gas convection) and $\alpha_{net} = 0.99955$ (dotted line, forced gas convection). The starting composition for each degassing trend was estimated based on the least degassed samples in each location.

powerful tracer of mantle recycling processes. In particular, it is worth noting that lavas from the HIMU (i.e., high U/Pb) OIB St. Helena generally display Tl isotope compositions lighter than the depleted mantle (Blusztajn et al., 2018), which clearly cannot be explained by degassing and was argued to be consistent with the presence of recycled altered oceanic crust in the mantle source. Regardless of the clear utility offered by Tl isotopes as a tracer of mantle recycling, it is also important to remember that it is near impossible to identify Tl isotope degassing effects for single samples from a volcano. Thus, we argue that future studies of subaerial lavas should focus on generating larger Tl isotope data sets for individual volcanic centers, which provides better means to identify possible effects from degassing. At the same time, subaerial lava data sets that feature single or only a few heavy Tl isotope compositions need to be carefully interpreted as it can be difficult to distinguish effects due to degassing from Tl isotope variation generated by distinct recycled sediment components.

5. Conclusions

We present new Tl isotope and concentration data for degassing experiments conducted in a 1 atm furnace. These exhibit Tl loss of 60%–90% relative to the starting material, which is accompanied by increasingly heavier Tl isotope compositions with increasing loss of Tl. The data are best accounted for by kinetic fractional isotope fractionation that is controlled primarily by diffusion under natural gas convection (Sossi et al., 2020) rather than under forced gas convection (Richter et al., 2002, 2011; Young et al., 2019). Our experimental results are consistent with TlCl being the primary species degassed, which is in agreement with evidence from natural volcanic systems (Churakov et al., 2000) and our own thermodynamic calculations. We calculate that degassing from natural systems should be associated with net Tl isotope fractionation factors of either $\alpha_{net} \sim 0.99969$ or $\alpha_{net} \sim 0.99955$ for diffusion in natural and forced gas convection cases, respectively.

We also present Tl isotope data for subaerial lavas from three Kamchatka arc volcanoes that broadly plot in between the predictions of the two degassing models. These results suggest that natural systems can operate under different degassing regimes, some of which approach forced gas convection with others approaching natural gas convection. However, an inspection of literature Tl isotope data for a range of OIBs and arc lavas reveal that only a minor subset of samples is likely to have been affected by degassing even at high degrees of magmatic evolution. It is presently unclear what processes are controlling the amount of Tl degassing and associated isotope fractionation in natural systems, but time exposure of the magma at atmospheric pressure and potentially diffusivity of Tl in the melt could be important factors.

Data Availability Statement

All data are included in the manuscript and are publicly available through the EarthChem database (https://doi.org/10.26022/IEDA/111790)

Acknowledgments
The authors thank Jérémy Guignard, Frank Richter, and Mathias Schannor and an anonymous reviewer for their constructive comments, which helped improve this manuscript significantly. The authors thank Janne Bichert-Toft for efficient editorial handling.

References

Andersen, M. B., Elliott, T., Freymuth, H., Sims, K. W. W., Niu, Y., & Kelley, K. A. (2015). The terrestrial uranium isotope cycle. *Nature*, *517*, 356–359. https://doi.org/10.1038/nature14062

Baker, R. G. A., Rehkämper, M., Hinkley, T. K., Nielsen, S. G., & Toutain, J. P. (2009). Investigation of thallium fluxes from subaerial volcanism—Implications for the present and past mass balance of thallium in the oceans. *Geochimica et Cosmochimica Acta*, *73*, 6340–6359. https://doi.org/10.1016/j.gca.2009.07.014

Barin, I., Sauert, F., Schultze-Rhonhof, E., & Sheng, W. S. (1989). *Thermochemical data of pure substances, Part I and Part II*. CH Verlagsgesellschaft.

Blusztajn, J., Nielsen, S. G., Marschall, H. R., Shu, Y., Ostrander, C. M., & Hanyu, T. (2018). Thallium isotope systematics in volcanic rocks from St. Helena – Constraints on the origin of the HIMU reservoir. *Chemical Geology*, *476*, 292–301. https://doi.org/10.1016/j.chemgeo.2017.11.025

Cabral, R. A., Jackson, M. G., Rose-Koga, E. F., Koga, K. T., Whitehouse, M. J., Antonelli, M. A., et al. (2013). Anomalous sulphur isotopes in plume lavas reveal deep mantle storage of Archaean crust. *Nature*, *496*, 490–493. https://doi.org/10.1038/nature12020

Chilton, T. H., & Colburn, A. P. (1934). Mass transfer (absorption) coefficients prediction from data on heat transfer and fluid friction. *Industrial & Engineering Chemistry Research*, *26*, 1183–1187. https://doi.org/10.1021/ie50299a012

Churakov, S. V., Tkachenko, S. I., Korzhinskii, M. A., Bocharnikov, R. E., & Shmulovich, K. I. (2000). Evolution of composition of high-temperature fumarolic gases from Kudryavy volcano, Iturup, Kuril Islands: The thermodynamic modeling. *Geochemistry International*, *38*, 436–451.

Churikova, T., Dorendorf, F., & Wörner, G. (2001). Sources and fluids in the mantle wedge below Kamchatka, evidence from across-arc geochemical variation. *Journal of Petrology*, *42*, 1567–1593. https://doi.org/10.1093/petrology/42.8.1567

Churikova, T., Wörner, G., Mironov, N., & Kronz, A. (2007). Volatile (S, Cl and F) and fluid mobile trace element compositions in melt inclusions: Implications for variable fluid sources across the Kamchatka arc. *Contributions to Mineralogy and Petrology*, *154*, 217–239. https://doi.org/10.1007/s00410-007-0190-z

Dorendorf, F., Churikova, T., Koloskov, A., & Wörner, G. (2000). Late Pleistocene to Holocene activity at Bakening volcano and surrounding monogenetic centers (Kamchatka): Volcanic geology and geochemical evolution. *Journal of Volcanology and Geothermal Research*, *104*, 131–151. https://doi.org/10.1016/s0377-0273(00)00203-1

Dorendorf, F., Wiechert, U., & Wörner, G. (2000). Hydrated sub-arc mantle: A source for the Kluchevskoy volcano, Kamchatka/Russia. *Earth and Planetary Science Letters*, *175*, 69–86. https://doi.org/10.1016/s0012-821x(99)00288-5

Foden, J., Sossi, P. A., & Nebel, O. (2018). Controls on the iron isotopic composition of global arc magmas. *Earth and Planetary Science Letters*, *494*, 190–201. https://doi.org/10.1016/j.epsl.2018.04.039

Freymuth, H., Vils, F., Willbold, M., Taylor, R. N., & Elliott, T. (2015). Molybdenum mobility and isotopic fractionation during subduction at the Mariana arc. *Earth and Planetary Science Letters*, *432*, 176–186. https://doi.org/10.1016/j.epsl.2015.10.006

Frössling, N. (1938). Uber die verdunstung fallernder tropfen. *Gerlands Beiträge zur Geophysik*, *52*, 170–216.

Gorbatov, A., Kostoglodov, V., Suárez, G., & Gordeev, E. (1997). Seismicity and structure of the Kamchatka subduction zone. *Journal of Geophysical Research*, *102*, 17883–17898. https://doi.org/10.1029/96jb03491

Hofmann, A. W. (1997). Mantle geochemistry: The message from oceanic volcanism. *Nature*, *385*, 219–229. https://doi.org/10.1038/385219a0

Hofmann, A. W., & White, W. M. (1982). Mantle plumes from ancient oceanic crust. *Earth and Planetary Science Letters*, *57*, 421–436. https://doi.org/10.1016/0012-821x(82)90161-3

Howarth, S., Prytulak, J., Little, S. H., Hammond, S. J., & Widdowson, M. (2018). Thallium concentration and thallium isotope composition of lateritic terrains. *Geochimica et Cosmochimica Acta*, *239*, 446–462. https://doi.org/10.1016/j.gca.2018.04.017

Huang, J., Zhang, X.-C., Chen, S., Tang, L., Wörner, G., Yu, H., & Huang, F. (2018). Zinc isotopic systematics of Kamchatka-Aleutian arc magmas controlled by mantle melting. *Geochimica et Cosmochimica Acta*, *238*, 85–101. https://doi.org/10.1016/j.gca.2018.07.012

Izbekov, P. E., Eichelberger, J. C., & Ivanov, B. V. (2004). The 1996 eruption of Karymsky volcano, Kamchatka: Historical record of basaltic replenishment of an andesite reservoir. *Journal of Petrology*, *45*, 2325–2345. https://doi.org/10.1093/petrology/egh059

Johnson, A., & Canil, D. (2011). The degassing behavior of Au, Tl, As, Pb, Re, Cd and Bi from silicate liquids: Experiments and applications. *Geochimica et Cosmochimica Acta*, *75*, 1773–1784. https://doi.org/10.1016/j.gca.2010.12.023

Le Roux, V., Dasgupta, R., & Lee, C.-T. A. (2011). Mineralogical heterogeneities in the Earth's mantle: Constraints from Mn, Co, Ni and Zn partitioning during partial melting. *Earth and Planetary Science Letters*, *307*, 395–408. https://doi.org/10.1016/j.epsl.2011.05.014

Liu, H., Xiao, Y., Sun, H., Tong, F., Heuser, A., Churikova, T., & Wörner, G. (2020). Trace elements and Li isotope compositions across the Kamchatka arc: Constraints on slab-derived fluid sources. *Journal of Geophysical Research: Solid Earth*, *125*, e2019JB019237. https://doi.org/10.1029/2019jb019237

Münker, C., Wörner, G., Yogodzinski, G., & Churikova, T. (2004). Behaviour of high field strength elements in subduction zones: Constraints from Kamchatka-Aleutian arc lavas. *Earth and Planetary Science Letters*, *224*, 275–293. https://doi.org/10.1016/j.epsl.2004.05.030

Makishima, A., & Nakamura, E. (2006). Determination of major/minor and trace elements in silicate samples by ICP-QMS and ICP-SFMS applying isotope dilution-internal standardisation (ID-IS) and multi-stage internal standardisation. *Geostandards and Geoanalytical Research*, *30*, 245–271. https://doi.org/10.1111/j.1751-908x.2006.tb01066.x

Moynier, F., Fujii, T., Brennecka, G. A., & Nielsen, S. G. (2013). Nuclear field shift in natural environments. *Comptes Rendus Geoscience*, *345*, 150–159. https://doi.org/10.1016/j.crte.2013.01.004

Nielsen, S. G., Horner, T. J., Pryer, H. V., Blusztajn, J., Shu, Y., Kurz, M. D., & Le Roux, V. (2018). Barium isotope evidence for pervasive sediment recycling in the upper mantle. *Science Advances*, *4*, eaas8675. https://doi.org/10.1126/sciadv.aas8675

Nielsen, S. G., Klein, F., Kading, T., Blusztajn, J., & Wickham, K. (2015). Thallium as a tracer of fluid-rock interaction in the shallow mariana forearc. *Earth and Planetary Science Letters*, *430*, 416–426. https://doi.org/10.1016/j.epsl.2015.09.001

Nielsen, S. G., Prytulak, J., Blusztajn, J., Shu, Y., Auro, M., Regelous, M., & Walker, J. (2017). Thallium isotopes as tracers of recycled materials in subduction zones: Review and new data for lavas from Tonga-Kermadec and Central America. *Journal of Volcanology and Geothermal Research*, *339*, 23–40. https://doi.org/10.1016/j.jvolgeores.2017.04.024

Nielsen, S. G., & Rehkämper, M. (2011). Thallium isotopes and their application to problems in earth and environmental science. In M. Baskaran (Ed.),, Ed., *Handbook of environmental isotope geochemistry* (pp. 247–269). Springer. https://doi.org/10.1007/978-3-642-10637-8_13

Nielsen, S. G., Rehkämper, M., Baker, J., & Halliday, A. N. (2004). The precise and accurate determination of thallium isotope compositions and concentrations for water samples by MC-ICPMS. *Chemical Geology*, *204*, 109–124. https://doi.org/10.1016/j.chemgeo.2003.11.006

Nielsen, S. G., Rehkämper, M., Brandon, A. D., Norman, M. D., Turner, S., & O'Reilly, S. Y. (2007). Thallium isotopes in Iceland and Azores lavas – Implications for the role of altered crust and mantle geochemistry. *Earth and Planetary Science Letters*, *264*, 332–345. https://doi.org/10.1016/j.epsl.2007.10.008

Nielsen, S. G., Rehkämper, M., Norman, M. D., Halliday, A. N., & Harrison, D. (2006). Thallium isotopic evidence for ferromanganese sediments in the mantle source of Hawaiian basalts. *Nature*, *439*, 314–317. https://doi.org/10.1038/nature04450

Nielsen, S. G., Rehkämper, M., Porcelli, D., Andersson, P., Halliday, A. N., Swarzenski, P. W., et al. (2005). Thallium isotope composition of the upper continental crust and rivers—An investigation of the continental sources of dissolved marine thallium. *Geochimica et Cosmochimica Acta*, *69*, 2007–2019. https://doi.org/10.1016/j.gca.2004.10.025

Nielsen, S. G., Rehkämper, M., & Prytulak, J. (2017). Investigation and application of thallium isotope fractionation. *Reviews in Mineralogy and Geochemistry*, *82*. https://doi.org/10.2138/rmg.2017.82.18

Nielsen, S. G., Rehkämper, M., Teagle, D. A. H., Butterfield, D. A., Alt, J. C., & Halliday, A. N. (2006). Hydrothermal fluid fluxes calculated from the isotopic mass balance of thallium in the ocean crust. *Earth and Planetary Science Letters*, *251*, 120–133. https://doi.org/10.1016/j.epsl.2006.09.002

Nielsen, S. G., Shimizu, N., Lee, C.-T. A., & Behn, M. D. (2014). Chalcophile behavior of thallium during MORB melting and implications for the sulfur content of the mantle. *Geochemistry, Geophysics, Geosystems*, *15*, 4905–4919. https://doi.org/10.1002/2014gc005536

Nielsen, S. G., Wasylenki, L. E., Rehkämper, M., Peacock, C. L., Xue, Z., & Moon, E. M. (2013). Toward an understanding of thallium isotope fractionation during adsorption to manganese oxides. *Geochimica et Cosmochimica Acta*, *117*, 252–265. https://doi.org/10.1016/j.gca.2013.05.004

Nielsen, S. G., Yogodzinski, G., Prytulak, J., Plank, T., Kay, S. M., Kay, R. W., et al. (2016). Tracking along-arc sediment inputs to the Aleutian arc using thallium isotopes. *Geochimica et Cosmochimica Acta*, *181*, 217–237. https://doi.org/10.1016/j.gca.2016.03.010

Noll, P. D., Newsom, H. E., Leeman, W. P., & Ryan, J. G. (1996). The role of hydrothermal fluids in the production of subduction zone magmas: Evidence from siderophile and chalcophile trace elements and boron. *Geochimica et Cosmochimica Acta*, *60*, 587–611. https://doi.org/10.1016/0016-7037(95)00405-x

Norris, C. A., & Wood, B. J. (2017). Earth's volatile contents established by melting and vaporization. *Nature*, *549*, 507–510. https://doi.org/10.1038/nature23645

Ponomareva, V., Melekestsev, I., Braitseva, O., Churikova, T., Pevzner, M., & Sulerzhitsky, L. (2007). Late Pleistocene-Holocene volcanism on the Kamchatka Peninsula, Northwest Pacific region,*Volcanism and subduction* (pp. 165–198). The Kamchatka Region. https://doi.org/10.1029/172gm15

Ponomareva, V., Portnyagin, M., Derkachev, A., Pendea, I. F., Bourgeois, J., Reimer, P. J., et al. (2013). Early Holocene M~6 explosive eruption from Plosky volcanic massif (Kamchatka) and its tephra as a link between terrestrial and marine paleoenvironmental records. *International Journal of Earth Sciences*, *102*, 1673–1699. https://doi.org/10.1007/s00531-013-0898-0

Prytulak, J., Brett, A., Webb, M., Plank, T., Rehkämper, M., Savage, P. S., & Woodhead, J. (2017). Thallium elemental behavior and stable isotope fractionation during magmatic processes. *Chemical Geology*, *448*, 71–83. https://doi.org/10.1016/j.chemgeo.2016.11.007

Prytulak, J., Nielsen, S. G., Plank, T., Barker, M., & Elliott, T. (2013). Assessing the utility of thallium and thallium isotopes for tracing subduction zone inputs to the Mariana arc. *Chemical Geology*, *345*, 139–149. https://doi.org/10.1016/j.chemgeo.2013.03.003

Rehkämper, M., Frank, M., Hein, J. R., & Halliday, A. (2004). Cenozoic marine geochemistry of thallium deduced from isotopic studies of ferromanganese crusts and pelagic sediments. *Earth and Planetary Science Letters*, *219*, 77–91. https://doi.org/10.1016/s0012-821x(03)00703-9

Rehkämper, M., Frank, M., Hein, J. R., Porcelli, D., Halliday, A., Ingri, J., & Liebetrau, V. (2002). Thallium isotope variations in seawater and hydrogenetic, diagenetic, and hydrothermal ferromanganese deposits. *Earth and Planetary Science Letters*, *197*, 65–81. https://doi.org/10.1016/s0012-821x(02)00462-4

Rehkämper, M., & Halliday, A. N. (1999). The precise measurement of Tl isotopic compositions by MC-ICPMS: Application to the analysis of geological materials and meteorites. *Geochimica et Cosmochimica Acta*, *63*, 935–944. https://doi.org/10.1016/s0016-7037(98)00312-3

Richter, F. M., Davis, A. M., Ebel, D. S., & Hashimoto, A. (2002). Elemental and isotopic fractionation of Type B calcium-, aluminum-rich inclusions: Experiments, theoretical considerations, and constraints on their thermal evolution. *Geochimica et Cosmochimica Acta*, *66*, 521–540. https://doi.org/10.1016/s0016-7037(01)00782-7

Richter, F. M., Mendybaev, R. A., Christensen, J. N., Ebel, D., & Gaffney, A. (2011). Laboratory experiments bearing on the origin and evolution of olivine-rich chondrules. *Meteoritics & Planetary Science*, *46*, 1152–1178. https://doi.org/10.1111/j.1945-5100.2011.01220.x

Ryan, J. G., & Chauvel, C. (2014). The subduction-zone filter and the impact of recycled materials on the evolution of the mantle. In H. D. H. K. Turekian (Ed.),, Ed., *Treatise on geochemistry* (2nd ed., pp. 479–508). Elsevier. https://doi.org/10.1016/b978-0-08-095975-7.00211-4

Schauble, E. A. (2007). Role of nuclear volume in driving equilibrium stable isotope fractionation of mercury, thallium, and other very heavy elements. *Geochimica et Cosmochimica Acta*, *71*, 2170–2189. https://doi.org/10.1016/j.gca.2007.02.004

Shu, Y., Nielsen, S. G., Marschall, H. R., John, T., Blusztajn, J., & Auro, M. (2019). Closing the loop: Subducted eclogites match thallium isotope compositions of ocean island basalts. *Geochimica et Cosmochimica Acta*, *250*, 130–148. https://doi.org/10.1016/j.gca.2019.02.004

Shu, Y., Nielsen, S. G., Zeng, Z., Shinjo, R., Blusztajn, J., Wang, X., & Chen, S. (2017). Tracing subducted sediment inputs to the Ryukyu arc-Okinawa trough system: Evidence from thallium isotopes. *Geochimica et Cosmochimica Acta*, *217*, 462–491. https://doi.org/10.1016/j.gca.2017.08.035

Sobolev, A. V., Asafov, E. V., Gurenko, A. A., Arndt, N. T., Batanova, V. G., Portnyagin, M. V., et al. (2019). Deep hydrous mantle reservoir provides evidence for crustal recycling before 3.3 billion years ago. *Nature*, *571*, 555–559. https://doi.org/10.1038/s41586-019-1399-5

Sossi, P. A., Moynier, F., Treilles, R., Mokhtari, M., Wang, X., & Siebert, J. (2020). An experimentally-determined general formalism for evaporation and isotope fractionation of Cu and Zn from silicate melts between 1300 and 1500 °C and 1 bar. *Geochimica et Cosmochimica Acta*, *288*, 316–340. https://doi.org/10.1016/j.gca.2020.08.011

Thomas, R. W., & Wood, B. J. (2021). The chemical behaviour of chlorine in silicate melts. *Geochimica et Cosmochimica Acta*, *294*, 28–42. https://doi.org/10.1016/j.gca.2020.11.018

Tolstykh, M. L., Naumov, V. B., Gavrilenko, M. G., Ozerov, A. Y., & Kononkova, N. N. (2012). Chemical composition, volatile components, and trace elements in the melts of the Gorely volcanic center, Southern Kamchatka: Evidence from inclusions in minerals. *Geochemistry International*, *50*, 522–550. https://doi.org/10.1134/s0016702912060079

Young, E. D., Shahar, A., Nimmo, F., Schlichting, H. E., Schauble, E. A., Tang, H., & Labidi, J. (2019). Near-equilibrium isotope fractionation during planetesimal evaporation. *Icarus*, *323*, 1–15. https://doi.org/10.1016/j.icarus.2019.01.012